Shew, R. L., & Deamer, D W. (1985) *Biochim. Biophys. Acta 816*, 1–8.
Small, D. (1967) *J. Lipid Res. 8*, 551–557.
Szoka, F. C., & Papahadjopoulos, D. (1978) *Proc. Natl. Acad. Sci. U.S.A. 75*, 4194–4198.
Szoka, F. C., & Papahadjopoulos, D. (1981) in *Liposomes: from Physical Structure to Therapeutic Applications* (Knight, C. G., Ed.) pp 51–79, Elsevier/North-Holland, New York.
Szoka, F. C., Olson, F., Heath, T., Vail, W. J., Mayhew, E., & Papahadjopoulos, D. (1980) *Biochim. Biophys. Acta 601*, 559–571.
Tardieu, A., Luzzati, V., & Reman, F. C. (1973) *J. Mol. Biol. 75*, 711–733.

Lipid Mobility and Order in Bovine Rod Outer Segment Disk Membranes. A Spin-Label Study of Lipid–Protein Interactions

Robert D. Pates[‡] and Derek Marsh*

Max-Planck-Institut für biophysikalische Chemie, Abteilung Spektroskopie, D-3400 Göttingen, Federal Republic of Germany

Received July 7, 1986; Revised Manuscript Received September 17, 1986

ABSTRACT: Lipid–protein interactions in bovine rod outer segment disk membranes have been studied by using a series of eight stearic acid spin-label probes which were labeled at different carbon atom positions in the chain. In randomly oriented membrane dispersions, the electron spin resonance (ESR) spectra of the C-8, C-9, C-10, C-11, C-12, C-13, and C-14 atom positional isomers all apparently consist of two components. One of the components corresponds closely to the spectra obtained from dispersions of the extracted membrane lipids, and the other, which is characterized by a considerably greater degree of motional restriction of the lipid chains, is induced by the presence of the protein. Digital subtraction has been used to separate the two components. The proportion of the motionally restricted lipid component is approximately constant, independent of the position of the spin-label group, and corresponds to 30–40% of the total spin-label spectral intensity. The hyperfine splitting of the outer maxima in the difference spectra of the motionally restricted component decreases, and concomitantly, the line widths increase with increasing temperature but change relatively little with increasing distance of the spin-label group from the polar head-group region. This indicates that the corresponding chain motions of the protein-interacting lipids lie in the slow-motion regime of spin-label ESR spectroscopy ($\tau_R \sim 10^{-8}$ s) and that the mobility of these lipids increases with increasing temperature but does not vary greatly along the length of the chain. The data from the hyperfine splittings also suggest the existence of a polarity gradient immediately adjacent to the protein surface, as observed in the fluid lipid regions of the membrane. The more fluid lipid component is only slightly perturbed relative to the lipids alone (for label positions 5–14, inclusive), indicating the presence of chain motions on the nanosecond time scale, and the spectra also reveal a similar polarity profile in both lipid and membrane environments. ESR spectra have also been obtained as a function of magnetic field orientation with oriented membrane samples. For the C-14 atom positional isomer, the motionally restricted component is observed to have a large hyperfine splitting, with the magnetic field oriented both parallel and perpendicular to the membrane normal. This indicates that the motionally restricted lipid chains have a broad distribution of orientations at this label position. A motionally restricted lipid component is also detected with the C-5 atom positional isomer in oriented membranes. It is concluded that the spin-labeled lipids in direct association with rhodopsin are not highly ordered and display motional restriction along the entire length of their chains, with rotational correlation times in the range of 10 ns.

Electron spin resonance (ESR)[1] spectroscopic measurements on a variety of different biological membranes and reconstituted lipid–protein systems have revealed the presence of two populations of spin-labeled lipids, differing in their molecular mobility. One population corresponds to the fluid environment typical of lipid bilayers, and the other, more motionally restricted component, is assigned to the lipid population interacting directly with the integral membrane proteins [see, e.g., Marsh & Watts (1982a)]. The effective number of motionally restricted lipids per protein is independent of the total lipid to protein ratio, if allowance is made for protein–protein contacts at low lipid/protein ratios. In this sense, the motionally restricted lipid may be defined as a first-shell or boundary layer (Jost et al., 1973a) of lipids interacting directly with the intramembranous surface of the protein.

The ESR spin-label method has proved very useful in analyzing both the stoichiometry and specificity of the lipid interactions with the surface of integral proteins in a wide variety of membrane systems. The effective number of

[‡] Present address: Department of Chemistry, University of Virginia, Charlottesville, VA 22901. Recipient of postdoctoral fellowship support from the American Heart Association.

[1] Abbreviations: ESR, electron spin resonance; ROS, rod outer segment(s); *n*-SASL, *n*-(4,4-dimethyloxazolidine-*N*-oxyl)stearic acid; *n*-PCSL, 1-acyl-2-[*n*-(4,4-dimethyloxazolidine-*N*-oxyl)stearoyl]-*sn*-glycero-3-phosphocholine; BHT, butylated hydroxytoluene; EDTA, ethylenediaminetetraacetic acid; HEPES, *N*-(2-hydroxyethyl)piperazine-*N*′-2-ethanesulfonic acid; Tris, tris(hydroxymethyl)aminomethane.

0006-2960/87/0426-0029$01.50/0

motionally restricted lipids correlates roughly with the known dimensions of the proteins, and specific selectivity patterns, particularly for negatively charged lipids, are found for the different proteins [see Marsh (1985) for a recent review]. However, much less is known about the structure, or ordering, and mobility of these first-shell lipids. Such features will be of particular importance with regard to the sealing of the protein into the membrane and for its interfacing and coupling with the fluid lipid environment, which is necessary in many cases for the efficient functioning of the protein [see, e.g., O'Brien et al. (1977), Baldwin & Hubbell (1985), and Sandermann (1978, 1986)].

Nuclear magnetic resonance of lipid–protein systems, on the other hand, has revealed lipid spectra consisting of a single component, which are characterized primarily by an increase in line broadening relative to the pure lipids (Seelig et al., 1982; Bloom & Smith, 1985; Pates et al., 1986). These results have been interpreted as indicating that the lipid exchange at the protein surface is intermediate between the characteristic time scales of the ESR and NMR spectroscopies. This would be the case, if the exchange were comparable in rate to the translational diffusion in fluid lipid bilayers [see, e.g., Vaz et al. (1985)]. Recent ESR measurements of the exchange rate are in complete agreement with this suggestion (Davoust et al., 1983; Horvath et al., unpublished results; Ryba et al., 1987). The finding that the main effects of the protein are on the resonance line widths, with little change in the ^2H quadrupole splittings or ^{31}P chemical shift anisotropies, suggests that the lipid motions are slowed down by the protein, but with little change in the molecular ordering. This is found to be in good agreement with the spin-label ESR studies on lipid–protein interactions with rhodopsin, which are reported here.

Rod outer segment (ROS) disk membranes present several advantages for a detailed study of lipid–protein interactions in biological membranes. These are a natural membrane system in which up to 90% of the total membrane protein is a single molecular species, the photoreceptor rhodopsin (Papermaster et al., 1976). The other membrane proteins are mostly peripheral, and thus, integral protein–lipid interactions in the disk membrane are almost exclusively with rhodopsin. It is thought that the rhodopsin molecule is present in the membrane as a monomer (Ebrey, 1971; Brett & Findlay, 1979), hence offering the maximum availability of the intramembranous surface for interaction with lipids. The membrane lipids are in a fluid state (Rousselet & Devaux, 1978; Favre et al., 1979; Miljanich et al., 1985), which allows rapid rotation (Cone, 1972; Baroin et al., 1977) and translation (Poo & Cone, 1973) of rhodopsin within the membrane. Thus, any possible complications of protein aggregation or lipid phase separation are avoided. In addition, the study of lipid–protein interactions in this system could shed light on the possible functional role of lipids in the visual cycle of rhodopsin (O'Brien et al., 1977; Baldwin & Hubbell, 1985).

Previous spin-label studies on ROS disk membranes have revealed the presence of a motionally restricted spin-labeled lipid population in addition to the usual fluid lipid component (Watts et al., 1979; Marsh et al., 1982; Pates et al., 1985). Although previously there has been some controversy in the literature, there is now a considerable measure of agreement that this motionally restricted component corresponds to those lipids which are interacting directly with nonaggregated rhodopsin (Watts et al., 1981). In the present work, we attempt to give a more detailed description of the structural and motional characteristics of these protein-interacting lipids. This has been done by investigating a series of spin-label isomers which are labeled at different positions in the lipid chain and by performing angular-dependent measurements on oriented membrane samples. The different label positional isomers together with the temperature dependence give information on the mobility and motional modes of the lipid chains, and the angular dependence gives information on the orientational distribution of the motionally restricted lipid chains. It is concluded that the lipids interacting directly with rhodopsin are not highly ordered and have segmental motions, the rotational correlation times of which lie in the region of 10 ns.

Materials and Methods

Preparation and Characterization of Rod Outer Segments. Cattle eyes were obtained from a local slaughterhouse in batches of 60. The retinas were removed by cutting the eye in half, turning the posterior region inside out, and carefully scraping the retina to the blind spot, where it was conveniently cut and transferred to 30 mL of standard buffer or 0.5 mL per retina (125 mM NaCl, 3.5 mM KCl, 1 mM $CaCl_2$, 1 mM $MgCl_2$, 0.5 mM EDTA, and 15 mM HEPES, pH 7.3). The retinas were shaken vigorously and filtered through gauze of pore diameter 30 μm, yielding 30–50 mL of crude ROS extract. This was divided into six aliquots and layered on a sucrose step gradient (1.14 specific gravity, sucrose dissolved in standard buffer). The gradients were centrifuged at 40000g in a Beckman SW27 rotor for 25 min. The ROS were harvested from the interface, washed 3 times in water to lyse the plasma membranes, and suspended in 8 mL of standard buffer. Absorption spectroscopy was routinely performed on the preparations and revealed that the yield of rhodopsin was between 7 and 20 nmol per retina and the A_{280}/A_{500} ratio was 2.3. The lipid/protein ratio of the preparations was determined to be 61 mol/mol, assuming a molecular weight of 39 000 for rhodopsin and a mean phospholipid molecular weight of 770. Protein and lipid phosphorus determinations were performed according to Lowry et al. (1956) and Eibl and Lands (1969), respectively.

Spin-Labels and Sample Preparation for ESR. Full details of the synthesis of stearic acid and *sn*-2 spin-labeled phospholipids are reported elsewhere (Marsh & Watts, 1982a). The spin-labels were stored at −20 °C in chloroform at a concentration of 1 mg/mL.

Wherever possible, spin-labeling was performed from ethanolic solution. The protein concentration of the sample to be labeled (typically 10 nmol of rhodopsin total) was determined from absorption spectroscopy, and the phospholipid content was calculated on the basis of 61 phospholipids per rhodopsin molecule. The spin-label (1.5 mol % of the endogenous lipid content) was then dried in a stream of nitrogen and kept under vacuum for 1 h. Pure ethanol (2–5 μL) was then added and the tube vortexed and incubated at 35 °C for 5 min. The ROS disk membrane suspension was then added in the dark in a volume of not less than 250 μL standard buffer to ensure that the ethanol concentration would never exceed 1%. The tube was vortexed immediately, followed by a further incubation at 35 °C. Samples containing stearic acid spin-labels were then pelleted in a 100-μL hematocrit tube and transferred to a darkened ESR laboratory for ESR measurements. Because of the tendency for the phospholipid spin-labels to form vesicles in aqueous solution, samples labeled with these probes were washed several times before transfer to hematocrit tubes for ESR measurements.

ROS lipid extracts in chloroform were labeled by the addition of 1 mol % spin-label in chloroform. Organic solvent was removed by evaporation in a stream of argon and then

under vacuum for several hours, prior to dispersion of the lipid in buffer and concentration in the ESR capillary by centrifugation.

Lipid Extraction. Lipids were extracted by using a modified version of the procedure of Folch et al. (1957). ROS (300 nmol of rhodopsin) were suspended in standard buffer containing a 10-fold molar excess of hydroxylamine to rhodopsin. The membranes were then thoroughly bleached on ice and pelleted in a Beckman 30 rotor, and the buffer was removed. While a jet of argon was played on the bleached membrane pellet, 0.5 mL of methanol/mg of lipid present in the sample was introduced and vortex-mixed with the membranes. The tube contents were then transferred to a glass bench-top centrifuge tube with a screw cap containing 2 volumes of chloroform. The chloroform contained butylated hydroxytoluene (BHT) such that the final concentration was 1 mol of BHT/200 mol of phospholipid. Standard buffer (0.2 volume of the total) was then added and mixed thoroughly, and the tube was centrifuged at 3000 rpm for 10 min. Two clear layers were separated, and the solid debris was collected at the interface. The upper phase was removed by suction, and the solid debris was carefully removed with a spatula. an equal volume of standard buffer was added to the lower phase to wash. The resulting chloroform phase was then concentrated in a stream of argon and stored at −20 °C.

Thin-layer chromatography demonstrated the presence of the three main lipid constituents, phosphatidylcholine, phosphatidylethanolamine, and phosphatidylserine, in the lipid extract. Analysis of the fatty acid methyl esters by gas–liquid chromatography gave a lipid chain composition similar to that reported by Stone et al. (1979). In particular, polyunsaturated fatty acids constituted 65% of the total, indicating negligible lipid peroxidation. Proton dipolar decoupled 109-MHz ^{31}P NMR spectra of coarse lipid dispersions in standard buffer indicated that the phospholipids were organized principally in a lamellar bilayer configuration. For some preparations, an isotropic and/or an inverted hexagonal lipid signal was observed, but when present, this was only appreciable at temperatures greater than 30 °C.

Preparation of Oriented Samples. Freshly lysed samples of ROS were labeled from ethanol as described above. The spin-labeled material (volume approximately 500 μL) was then carefully floated on high ionic strength buffer (200 mM NaCl, 150 mM KCl, 10 mM $MgCl_2$, 10 mM $CaCl_2$, 10 mM LiCl, 1 mM EDTA, and 50 mM Tris, pH 7.3) in a Beckman SW41 cellulose nitrate centrifuge tube, which contained a homemade Teflon insert 1 cm long. The insert had been carefully machined so as to fit neatly into the tube base, and the upper surface was planar and carried a piece of mica whose upper face had been roughened, and which was adhered to the planar surface by means of a small amount of laboratory grease. The membranes were centrifuged onto the mica at 200000*g*. The buffer was removed in the dark, the tube cut down to the insert, and the mica sheet plus oriented ROS film carefully detached with fine forceps. The mica was carefully trimmed and inserted into a Varian ESR tissue cell which was sealed by using laboratory grease. The cell was inserted into a horizontally mounted ESR cavity, and spectra were recorded in the dark.

Partially oriented ROS lipid extracts were prepared by evaporation of spin-labeled lipid (10 μg/μL) in chloroform (300 μL) inside an ESR flat cell by passage of a gentle flow of dry nitrogen. The lipid dried as a smooth film on the glass surfaces of the flat cell, and traces of solvent were removed under vacuum. The multilayers of ROS were hydrated by filling the cell with standard buffer which was left in contact with the lipid for at least 2 h. The buffer was drained from the cell which was then sealed and inserted into a horizontally oriented ESR cavity for ESR measurements.

ESR Spectroscopy. ESR measurements were made by using a Varian E-12 9-GHz spectrometer equipped with a nitrogen gas-flow temperature regulation system. Samples sealed in capillary tubes as described above were accommodated within standard 4-mm quartz ESR tubes containing silicone oil for thermal stability. Temperatures were measured with a thermocouple placed inside the quartz tube, slightly above the cavity.

ESR spectra were recorded and stored digitally on disk via a PDP 11/10 dedicated computer. Spectral subtractions were performed by using programs written by W. Moeller of this Institute. The strategies used for spectral subtraction are described in Marsh and Watts (1982b). Apparent order parameters were calculated by using the expression

$$S_{app} = \frac{A_{\parallel} - A_{\perp}}{A_{zz} - \frac{1}{2}(A_{xx} + A_{yy})} \frac{a'_0}{a_0} \quad (1)$$

where $2A_{\parallel}$ is equal to the outer, maximum hyperfine splitting ($2A_{max}$) and $A_{\perp}$ is obtained from the inner, minimum hyperfine splitting ($2A_{min}$) according to (Griffith & Jost, 1976)

$$A_{\perp}(G) = A_{min}(G) + 1.4\left[1 - \frac{A_{\parallel} - A_{min}}{A_{zz} + \frac{1}{2}(A_{xx} + A_{yy})}\right] \quad (2)$$

The effective isotropic hyperfine splitting constant is given by

$$a_0 = \frac{1}{3}(A_{\parallel} + 2A_{\perp}) \quad (3)$$

and that corresponding to the single-crystal environment in which the principal values of the hyperfine tensor A_{xx}, A_{yy}, and A_{zz} were measured is given by $a'_0 = {}^1/_3(A_{xx} + A_{yy} + A_{zz})$. Recently, detailed line-shape simulations have shown that the spectra of lipid spin-labels in fluid bilayers contain important contributions from slow molecular motions (Lange et al., 1985). Thus, the effective order parameter calculated by using eq 1, which assumes fast motion, can only be considered as an apparent value but is nonetheless useful for making intercomparisons between membranes and lipid dispersions or between different membranes.

Results

Two-Component Spectra of the n-Positional Isomers. The ESR spectra from six of the eight stearic acid spin-label positional isomers studied are given in Figure 1. In each case, the spectrum from the label in ROS disk membranes is compared with that from the same label in an aqueous dispersion of the extracted membrane lipids. The temperature at which the spectra were recorded is chosen such as to give best resolution of the second, motionally restricted, spectral component which appears in the wings of the membrane spectra (indicated by the arrows in Figure 1). For the 14-SASL positional isomer, the membrane spectra at 3 °C contain very clear outer peaks with a splitting of approximately 61 G, in addition to an anisotropic fluid spectral component which is very similar to that obtained from the extracted lipids. For the 12-, 11-, and 10-SASL positional isomers, the motionally restricted component appears as shoulders in the wings of the fluid lipid component, rather than as completely resolved peaks, and the temperature for optimum resolution increases from 18 to 30 °C as the anisotropy of the fluid component increases. For the 8-SASL label, the motionally restricted component is no longer evident as shoulders but solely as increased intensity in the wings of the membrane spectra relative to the extracted lipids. For the 5-SASL label, the anisotropy of the fluid

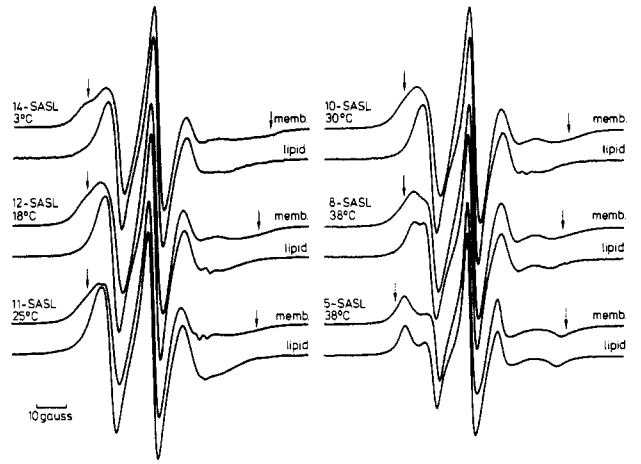

FIGURE 1: ESR spectra of the 14-, 12-, 11-, 10-, 8-, and 5-SASL stearic acid spin-label positional isomers in bovine ROS disk membranes (upper spectrum of each pair) and dispersions of the extracted membrane lipids (lower spectrum of each pair). The temperature at which each pair of spectra was recorded was adjusted to maximize the resolution of the motionally restricted component, which is indicated by the arrows in the wings of the membrane spectra.

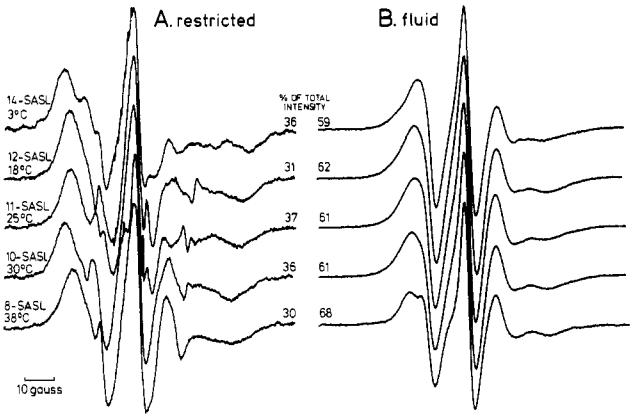

FIGURE 2: ESR difference spectra of the *n*-SASL stearic acid spin-label positional isomers in ROS membranes at the indicated temperatures. (A) Motionally restricted component obtained by subtraction of a lipid spectrum from the membrane spectrum. (B) Fluid component obtained by subtraction of a simulated motionally restricted component from the membrane spectrum. All spectra were normalized to the same central line height for this display. Percentages indicate the relative double -integrated intensity remaining in the difference spectra. For further details, see text.

component is so large that a second motionally restricted component can no longer be resolved in the membrane spectra, although a slight broadening is still evident in the outer wings. In this latter case, definitive evidence for the existence of the second component comes from studies with oriented samples, which are described later.

Spectral Subtraction. The two components in the membrane spectra have been resolved and quantitated by spectral subtraction. The resulting difference spectra are given in Figure 2. The motionally restricted and fluid component subtraction end points are given on the left-hand and right-hand sides of the figure, respectively. The motionally restricted component end points were obtained by subtracting the spectrum of the extracted lipids from that of the membranes. The lipid spectrum was chosen which best fitted the fluid component in the membrane spectrum. In general, this was a spectrum recorded at a somewhat lower temperature than the corresponding membrane spectrum. The fluid component end points were obtained by subtracting the same simulated slow-motion spectrum as was used by Watts et al. (1979) from the membrane spectrum. The simulated spectrum was for slow isotropic motion and was taken from Freed (1976). When necessary, the total width of the simulated spectrum was adjusted digitally to match that of the motionally restricted component in the membrane spectrum.

Table I: Fraction of Motionally Restricted Component, f_b, and Fraction of Fluid Component, f_f, in ESR Spectra of *n*-SASL Stearic Acid and *n*-PCSL Phosphatidylcholine Spin-Labels in Rod Outer Segment Disk Membranes[a]

label	f_b	$1 - f_f$	f_{mean}[b]
14-SASL	0.36	0.41	0.38
14-PCSL	0.30	0.40	0.35
13-SASL	0.31	0.37	0.34
12-SASL	0.31	0.38	0.35
12-PCSL	0.39	0.33	0.36
10-SASL	0.36	0.39	0.37
8-SASL	0.30	0.32	0.31
8-PCSL	0.31	0.34	0.32

[a] Obtained by spectral subtraction. [b] $f_{mean} = [f_b + (1 - f_f)]/2$.

The relative amounts of the two spectral components, obtained from double integration of the first-derivative spectra, are given in Table I. Results from phosphatidylcholine spin-label positional isomers, *n*-PCSL, are also included for comparison. It is seen from Table I that essentially consistent values for the fractions of motionally restricted (f_b) and fluid (f_f) lipid are obtained from the complementary subtractions which yield the difference spectra in Figure 2, panels A and B, respectively. Slight discrepancies between the two methods may arise because of the difficulty in obtaining exact fits to the single-component spectra, due at least in part to incipient effects of slow exchange between the two components (Horvath et al., unpublished results; Ryba et al., 1987). There is little difference between the values of f determined for the different positional isomers, and the results from the corresponding stearic acid and phosphatidylcholine spin-labels are also very similar. The latter is in accord with previous results which showed very little selectivity between the different lipids labeled on the C-14 position (Watts et al., 1979; Pates et al., 1985). The range of values for f_{mean} in Table I agrees very well with previous estimates for bovine ROS (Watts et al., 1979) and for frog rhodopsin (Pates et al., 1985) obtained by using different 14-positional isomer spin-labels.

Motionally Restricted Spin-Label Lipid Component. The spectra of the motionally restricted lipid components in Figure 2A lie in the slow-motional regime of ESR spectroscopy. This is seen from the temperature dependence of the outer hyperfine splitting, $2A_{max}$ and the line widths of the low-field and high-field outer extrema, ΔH_l and ΔH_h, respectively, given in Figure 3. The line splittings decrease and the line widths increase with increasing temperature, indicating the presence of chain mobility on the tens of nanoseconds time scale for all the positional isomers studied [see, e.g., Marsh (1986)]. Different temperature ranges are covered by the different positional isomers, and the data from the line widths all lie essentially on the same smooth curve (Figure 3B). The data for the line splittings, however, show discontinuities between the different positional isomers (Figure 3A). This is attributed to differences in polarity at the different spin-label locations, since these affect A_{max} (see below) but not the line widths.

Empirical calibrations for the line splittings and line widths, based on spectral simulations for slow isotropic rotational motion, have been given by Freed (1976). The expressions for the effective rotational correlation time, τ_R, are

$$\tau_R(A_{max}) = a(1 - A_{max}/A_{zz}^R)^b \quad (4)$$

$$\tau_R(\Delta H_m) = a_m(\Delta H_m/\Delta H_m^R - 1)^{b_m} \quad (5)$$

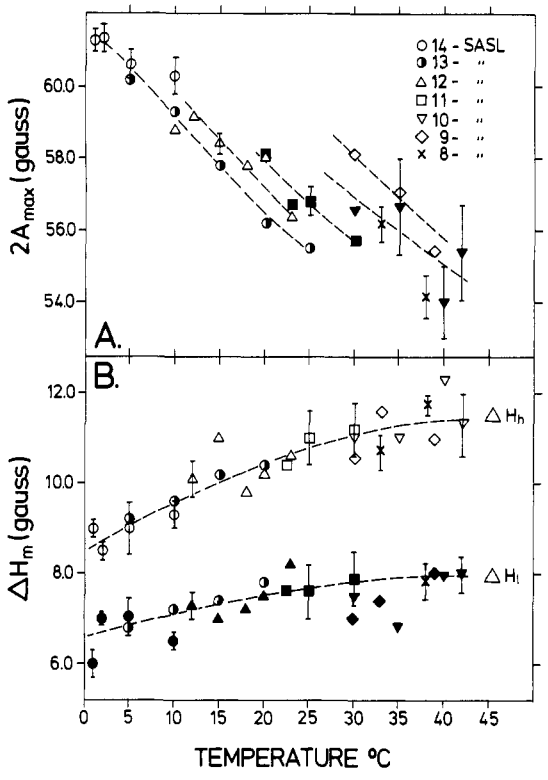

FIGURE 3: Temperature dependence of (A) the maximum outer hyperfine splitting, $2A_{max}$, and (B) the line widths of the low-field (closed symbols) and high-field (open symbols) outer hyperfine peaks, ΔH_l and ΔH_h, respectively, in the motionally restricted spectral components of the *n*-SASL stearic acid spin-label positional isomers in bovine ROS membranes. With the exception of 13-SASL, the open and closed symbols are used only for clarity in (A).

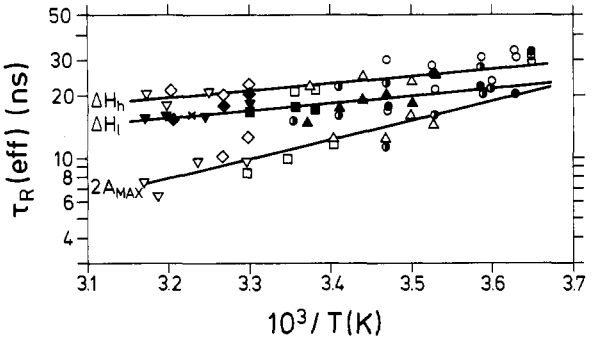

FIGURE 4: Arrhenius plot of the temperature dependence of the effective rotational correlation times derived from the outer hyperfine splitting, $2A_{max}$, and outer line widths, ΔH_l and ΔH_h, in the motionally restricted component of the *n*-SASL stearic acid spin-labels in bovine ROS membranes. Symbols are as defined in Figure 3.

where A_{zz}^R and ΔH_m^R are the rigid limit values of the hyperfine splitting constant, A_{max}, and outer line widths, ΔH_m, respectively. The values of the calibration constants for Brownian rotational diffusion are as follows: $a = 5.4 \times 10^{-10}$ s, $b = -1.36$; $a_l = 1.15 \times 10^{-8}$ s, $b_l = -0.943$; and $a_h = 2.12 \times 10^{-8}$ s, $b_h = -0.778$ (Freed, 1976). The temperature dependence of the effective correlation times obtained from these calibrations is given as an Arrhenius plot for the different spin-label positional isomers in Figure 4. There are small systematic differences between the effective correlation times obtained from the three different parameters, but all are rather similar and lie in the range $\tau_R \sim 10$–20 ns. The principal discrepancies arise with the correlation times deduced from A_{max}, since in this case the rigid limit values depend on polarity and therefore are more difficult to estimate. To a first approximation, the different correlation times display a single Arrhenius law temperature dependence, independent of positional isomer, with apparent activation energies of 1.5, 1.5, and 4.3 kcal/mol for the values deduced from ΔH_l, ΔH_h, and A_{max}, respectively.

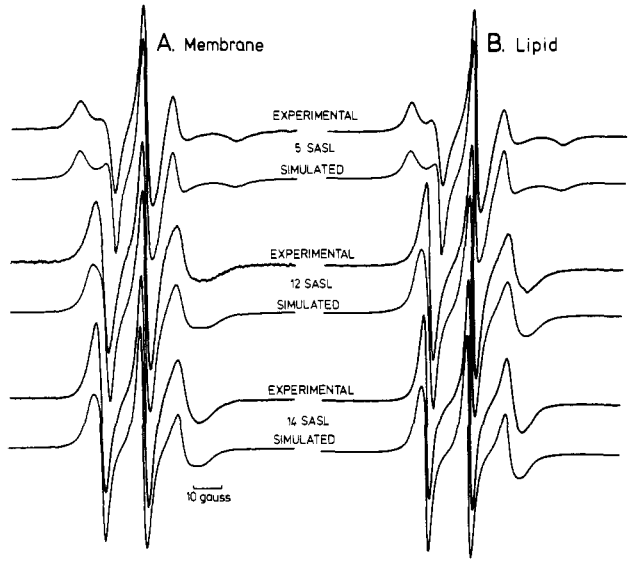

FIGURE 5: Experimental ESR spectra at 38 °C (upper spectrum of each pair) and simulated spectra using motional narrowing theory (lower spectrum of each pair) of the fluid component of the *n*-SASL stearic acid spin-label isomers in (A) ROS disk membranes (difference spectra) and (B) ROS disk extracted lipid dispersions. Simulations were obtained with the effective rotational correlation times given in Table II.

Table II: Effective Rotational Correlation Times [$\tau_{20} = \tau_{22}$ (ns)] Obtained from Simulations of Anisotropic Motion Assuming Motional Narrowing Theory (Schindler & Seelig, 1973) for Stearic Acid Spin-Labels, *n*-SASL, in Bovine ROS Disk Membranes (Fluid Component) and Dispersions of Extracted Membrane Lipids[a]

	effective rotational correlation time (ns)	
spin-label	membrane fluid component	extracted lipids
5-SASL	1.55 ± 0.1	1.25 ± 0.1
12-SASL	1.5 ± 0.1	1.2 ± 0.1
14-SASL	1.1 ± 0.1	0.8 ± 0.1

[a] $T = 38$ °C. Simulations are given in Figure 5.

Fluid Spin-Label Lipid Component. The fluid component difference spectra from ROS membranes are compared with the spectra of the same stearic acid spin-label isomers in the extracted membrane lipids in Figure 5. It is seen that the principal difference between the spectra is the increased line widths of the fluid lipid component in membranes compared with the extracted lipids, with relatively little change in line splittings. An attempt to quantitate this effect has been made by spectral simulations using motional narrowing theory (Schindler & Seelig, 1973). It is known from more comprehensive simulations using the stochastic Liouville equation that spin-labeled lipids in membranes have important dynamic modes in the slow-motional regime of ESR spectroscopy (Lange et al., 1985). However, the anisotropic motional narrowing theory provides a simple and rapid empirical approach to problems which at the moment are not immediately accessible to the more advanced methods. It is to be expected that this will yield effective correlation times which are biased toward the fastest molecular motion present (trans–gauche isomerization) but which are modulated by the presence of the components in the slow-motional regime (chain rotation and chain fluctuation). Simulations of the fluid component spectra made in this way are shown in Figure 5, and the values

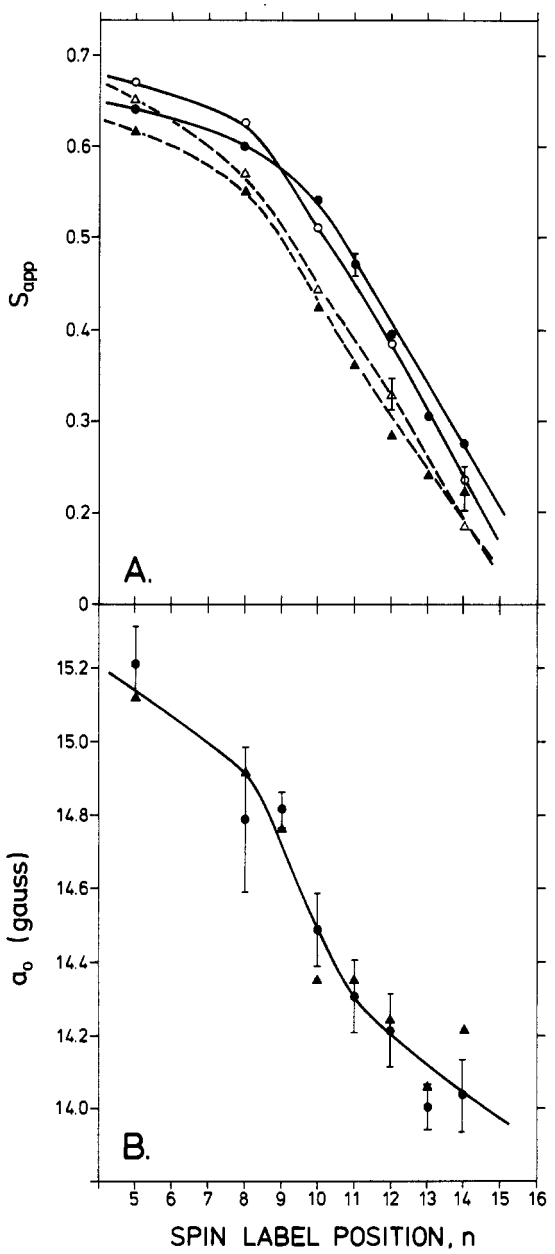

FIGURE 6: (A) Apparent order parameter profile of *n*-SASL stearic acid (closed symbols) and *n*-PCSL phosphatidylcholine (open symbols) spin-label positional isomers in bovine ROS membranes (○) and extracted lipid dispersions (△) at 20 °C. (B) Apparent isotropic hyperfine splitting factor profile of *n*-SASL spin-label positional isomers in bovine ROS disk membranes (●) and extracted lipid dispersions (▲).

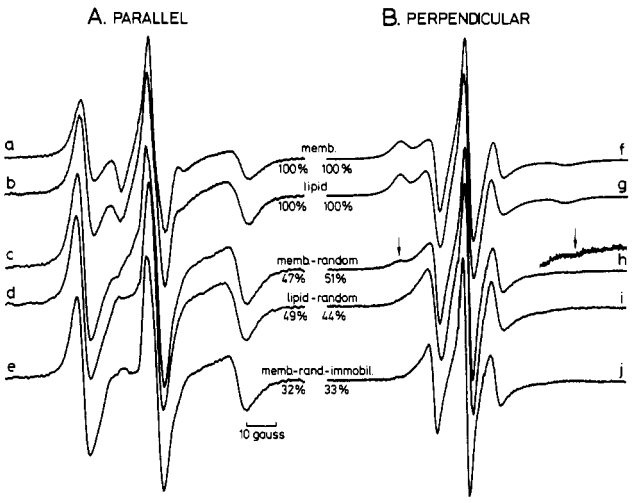

FIGURE 7: Experimental ESR spectra and difference spectra of the 5-SASL stearic acid spin-label in partially oriented bovine ROS disk membranes and extracted lipids at 20 °C. (A) Spectra recorded with the magnetic field oriented parallel to the substrate normal. (B) Spectra recorded with the magnetic field oriented perpendicular to the substrate normal. (a and f) Membrane spectra; (b and g) extracted lipid spectra; (c and h) membrane difference spectra with random component subtracted (motionally restricted component indicated by arrows); (d and i) lipid difference spectra with random component subtracted; (e and j) membrane double difference spectra with random and motionally restricted components subtracted. All spectra were normalized to the same central line height for this display. Percentages indicate the relative double-integrated intensity remaining in the difference spectra. For further details, see text.

of the effective rotational correlation times used for the simulations are given in Table II. It was assumed that the effective rate of molecular fluctuation perpendicular to the chain axis was equal to that for rotation about this axis, i.e., $\tau_{20} = \tau_{22}$ (Schindler & Seelig, 1973), consistent with trans–gauche isomerization being the dominant fast motion. The total residual line width used was 1.6 G in each case. For all three label positions, it is seen that the effective rotational correlation time for segmental chain motion is appreciably longer in the membranes than in the lipids alone. In both membranes and lipids, the effective correlation time changes very little until the C-14 atom position is reached, close to the end of the chain.

The apparent order parameters and isotropic hyperfine splitting constants of the fluid spin-label lipid component in membranes are compared with those in the extracted lipids in Figure 6. Although these can only be considered as effective values because of the possible breakdown of motional narrowing theory upon which eq 1 and 3 are based, they are nonetheless useful for making intercomparisons between membranes and lipids. Very similar apparent order parameter and a_0 profiles are obtained from both stearic acid and phosphatidylcholine spin-label positional isomers, indicating that both series of labels are intercalated similarly within the membrane. Similar profiles are also found for both membranes and the extracted lipid dispersions, indicating the presence of the characteristic fluid lipid bilayer permeability barrier in the membranes. Slightly larger apparent order parameters are found in membranes than in the extracted lipids. This could be due to a decreased rate of motion (in the slow regime) for the membranes relative to the lipids, however, rather than an increase in order per se. The apparent polarity profile, recorded by the isotropic hyperfine constant, a_0, is identical within experimental error for both membranes and lipid dispersions.

Oriented Membrane and Lipid Samples. The ESR spectra of the 5-SASL stearic acid spin-label in partially oriented membranes and extracted lipids, with the magnetic field oriented either parallel or perpendicular to the normal to the orienting substrate, are given in Figure 7a,b and Figure 7f,g, respectively. Using the techniques described under Materials and Methods, it was not possible to obtain fully hydrated membrane or lipid samples with a better degree of orientation than that indicated in Figure 7. A high degree of anisotropy is observed between the spectra with the magnetic field oriented parallel or perpendicular to the substrate normal, but in both cases, these are overlaid with the spectra from a randomly oriented component which presumably arises from unavoidable edge effects. The randomly oriented component cannot be totally distinguished from the effects of slow molecular motion, but it can be largely removed by spectral subtraction as indicated in Figure 7c, d and Figure 7h, i. The

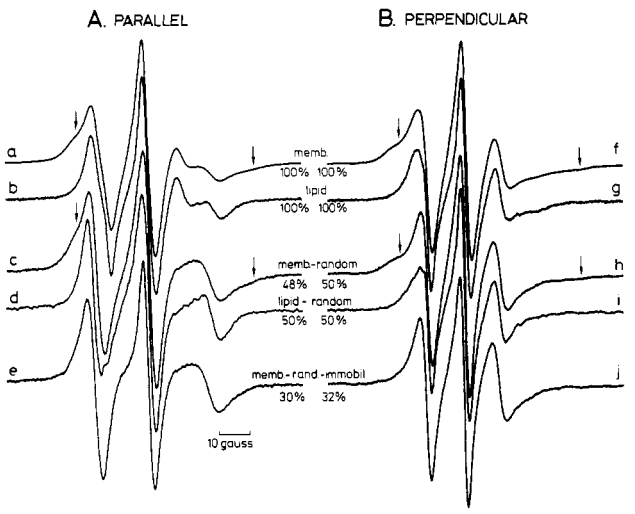

FIGURE 8: Experimental ESR spectra and difference spectra of the 14-SASL stearic acid spin-label in partially oriented bovine ROS disk membranes and extracted lipids at 11 °C. (A) Spectra recorded with the magnetic field oriented parallel to the substrate normal. (B) Spectra recorded with the magnetic field oriented perpendicular to the substrate normal. (a and f) Membrane spectra (motionally restricted component indicated by arrows); (b and g) extracted lipid spectra; (c and h) membrane difference spectra with the random component subtracted; (d and i) lipid difference spectra with the random component subtracted; (e and j) membrane double-difference spectra with the random and motionally restricted components subtracted. All spectra were normalized to the same central line height for this display. Percentages indicate the relative double-integrated intensity remaining in the difference spectra.

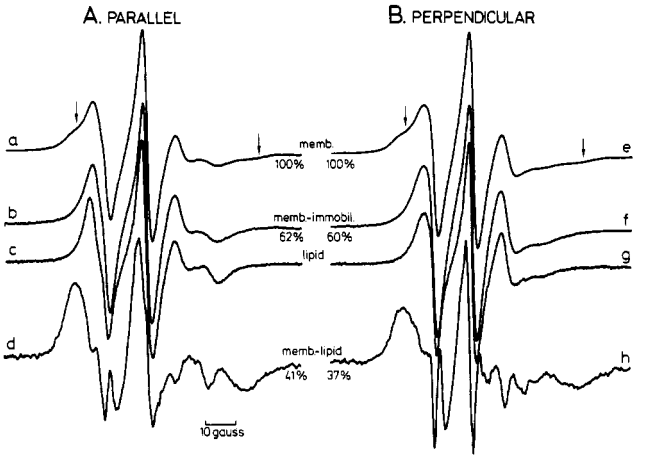

FIGURE 9: Alternative subtraction scheme to quantitate the motionally restricted component in the ESR spectra of the 14-SASL stearic acid spin-label in partially oriented ROS disk membranes at 10 °C. (A) Spectra recorded with the magnetic field oriented parallel to the substrate normal. (B) Spectra recorded with the magnetic field oriented perpendicular to the substrate normal. (a and e) Membrane spectra (motionally restricted component indicated by arrows); (b and f) membrane difference spectra with the motionally restricted component subtracted; (c and g) extracted lipid spectra; (d and h) membrane difference spectra with the lipid spectra subtracted. All spectra were normalized to the same central line height for this display. Percentages indicate the relative double-integrated intensity remaining in the difference spectra.

criterion used for the subtraction end points was that the individual hyperfine lines should, wherever possible, be symmetrical about the base line. Imperfections in the end points can most probably be attributed to the effects of slow motion. In this way, it was found that approximately 50% of the sample was well oriented in each case. Very similar subtraction factors were found for the spectra corresponding to both magnetic field directions, as might be expected.

Whereas in the subtraction for the lipids it was possible to remove completely the peaks in the outer wings of the spectrum with the perpendicular magnetic field orientation (Figure 7i), for the membrane spectra this was not possible. The peaks indicated by the arrows in Figure 7h therefore provide evidence for the existence of a motionally restricted lipid component in the spectra of the 5-SASL stearic acid spin-label in ROS membranes. This component is not resolved in the spectra for the parallel magnetic field orientation because of overlap with the fluid component which has a large hyperfine splitting for this orientation (Figure 7c, d). An important feature of the motionally restricted component is that, unlike the fluid component, it has an intensity corresponding to large hyperfine splittings (~58 G) in the spectra for the perpendicular magnetic field orientation (Figure 7h). Therefore, it is clear that the motionally restricted component must have a wide orientational distribution and not be highly oriented relative to the membrane normal (in which case a narrower splitting would have been observed for the perpendicular magnetic field orientation). The identity of the motionally restricted component was further substantiated by spectral subtraction. Subtracting a randomly oriented, motionally restricted component from the oriented membrane spectra in Figure 7c, h yielded the subtraction end points given in Figure 7e, j which correspond very closely to the spectra of the oriented lipids given in Figure 7d, i. The fraction of motionally restricted lipid required for the latter subtraction series was essentially the same for both magnetic field orientations (f_b = 0.32 and 0.35), as it should be. This value also lies within the range obtained for the various spin-label positional isomers in randomly oriented dispersions, given in Table I. The consisent subtraction obtained with the randomly oriented spectrum again suggests a wide angular distribution for the motionally restricted component.

The corresponding experimental and difference spectra to those given for the 5-SASL spin-label in Figure 7 are given for the 14-SASL stearic acid positional isomer in Figure 8. In this case, the spectral anisotropy is not so great as for the 5-positional isomer, and a motionally restricted component (indicated by the arrows in Figure 8a, f) can be detected in the spectra for both magnetic field orientations. The samples again contain appreciable amounts of randomly oriented material, and spectral subtraction again shows this to comprise approximately 50% of the total, as in the case of the 5-SASL experiment. The difference spectra corresponding to the oriented fraction of the membranes (Figure 8c, h) contain a motionally restricted component (indicated by the arrows), which is seen in the outer wings for both magnetic field orientations. Since the maximum splitting of the peaks from this component is approximately the same (~58 G) for both field orientations and similar to that found in randomly oriented samples, it may be concluded that the motionally restricted component for 14-SASL must also have a wide orientational distribution. As for 5-SASL, subtraction of a randomly oriented motionally restricted component from the oriented membrane spectra again yields difference spectra (Figure 8e, j) which strongly resemble the oriented lipid spectra (Figure 8d, i). The fraction of the motionally restricted component in the spectra of the oriented samples (f_b = 0.38 and 0.36) is in substantial agreement with the results from randomly oriented membrane dispersions in Table I, again in accord with the results from the 5-positional isomer.

The fact that the percentage of oriented material is approximately the same in both membrane and lipid samples allows an alternative strategy for spectral subtraction which is illustrated in Figure 9. Subtraction of approximately 40%

of the intensity from the spectra of the partially oriented membranes (Figure 9a, e), using a randomly oriented motionally restricted spectrum, yields subtraction end points (Figure 9b, f) whose line shapes are very similar to those of the partially oriented lipids (Figure 9c, g). Alternatively, subtraction of approximately 60% of the intensity from the partially oriented membrane spectra (Figure 9a, e), using the partially oriented lipid spectra (figure 9c, g), yields subtraction end points (Figure 9d, h) which correspond to the motionally restricted component. Thus, this alternative subtraction scheme again verifies that the fraction of motionally restricted lipid deduced from the spectra corresponding to both magnetic field orientations is similar (f_b = 0.41 and 0.37) and in accord with the values for randomly oriented membrane preparations (Table I). Although the difference spectra of Figure 9d, h contain some sharp spikes in the central region of the spectrum, probably arising from slight mismatches in the line widths and degree of misorientation of the lipid sample, the line shapes are very similar for both magnetic field orientations and correspond reasonably closely to a typical slow-motion spectrum from a randomly oriented sample. This again suggests that there is relatively little orientation dependence in the spectra of the motionally restricted component of 14-SASL in ROS membranes.

Discussion

The present work represents a rather complete experimental characterization of the spin-labeled lipid chain dynamics in ROS membranes. As in previous studies (Watts et al., 1979, 1981; Marsh et al., 1982; Pates et al., 1985), the results can be interpreted essentially in terms of two lipid components of differing mobility. One component is motionally restricted by direct interaction with the intramembranous section of the integral protein rhodopsin, and the other component has a mobility which is only little disturbed by the presence of the protein. These two components must, of course, be coupled by exchange of lipids on and off the intramembranous section of the protein. The new and significant features of the present work are the use of spin-labels positioned at a large variety of different locations down the lipid chain, an extensive study of the motional characteristics of the restricted lipid component, and the use of oriented samples.

Quantitation of the Two-Component Model. The spectra of all the different positional isomers in membranes can be interpreted in terms of the two-component model. If the results from the oriented samples are included, this includes C atoms from position 5 to position 14. The resolution of the two spectral components is difficult for the positional isomers with larger anisotropy in the fluid component, but the quality of the difference spectra of Figure 2 indicates that a uniform two-component model can be applied to the interpretation of the spectra from all label positions. The two components are likely to be coupled by exchange at the protein–lipid interface, and indeed, the exchange rate in both reconstituted rhodopsin systems (Davoust et al., 1983; Ryba et al., 1987) and ROS membranes (Pates et al., 1985; Marsh et al., 1982) has been estimated to be in the region of $\geq 10^7$ s^{-1}. Exchange at this rate is expected to have an effect on the individual spectral components, giving rise particularly to a broadening of the fluid component and a decrease in resolution of the two components (Davoust & Devaux, 1982; Horvath et al., unpublished results; Marsh, 1986). This could account, at least in part, for some of the sharp discontinuities seen in the motionally restricted difference spectra in Figure 2A and for the increase in the effective rotational correlation time of the fluid component in the membrane spectra (see Table II). It should be noted that the estimated exchange rates are such that, because of the difference in characteristic time scales between ESR and NMR, it is to be expected that a single, exchange-averaged spectrum would be expected in both ^2H and ^{31}P NMR studies. This seems to be the case for a wide variety of different lipid–protein systems in the fluid phase (Seelig et al., 1982; Kang et al., 1979; Bloom & Smith, 1985), including those containing rhodopsin (Bienvenue et al., 1982; Deese et al., 1981; Ellena et al., 1986; Pates et al., 1986).

The fractions of the motionally restricted component deduced from the different positional isomers and from oriented as well as random membrane dispersions all lie within the same range. It is also very significant that the same fraction of motionally restricted lipid was obtained from the spectra recorded with different magnetic field orientations for the oriented samples (cf. Figure 8). For exchange-coupled spectra, the broadening of the fluid component can affect the quantitation of the individual components. However, this can be largely compensated for by choosing individual spectral components which most closely correspond to the apparent components in the composite spectrum (Horvath et al., unpublished results; Marsh, 1985), e.g., by using a pure lipid spectrum recorded at a slightly lower temperature, as was done in the present study. The mean fraction of motionally restricted lipid obtained from all these measurements is then $f_b = 0.35 \pm 0.04$, where the limits correspond to the maximum range of observed values. Assuming no selectivity of the different lipids for rhodopsin ($K_r = 1$; Watts et al., 1979), the number of motionally restricted lipids, N_l, associated with each protein is obtained from

$$n_f^*/n_b^* = n_t/N_l - 1 \qquad (6)$$

where $n_f^*/n_b^* = (1 - f_b)/f_b$ is the ratio of fluid to motionally restricted components in the ESR spectrum. The lipid to protein ratio of the ROS membrane preparations is $n_t = 61$ phospholipids per 39 000-dalton protein, yielding a value of $N_l = 21 \pm 3$ motionally restricted lipids per rhodopsin. From the available dimensional data, Pates et al. (1985) concluded that approximately 24 phospholipids could be accommodated around the monomeric rhodopsin molecule. This value correlates well with the number of motionally restricted lipids interacting with rhodopsin, confirming as suggested previously (Watts et al., 1979; Pates et al., 1985) that these may constitute the first shell of lipids surrounding the protein. From the measured lipid to protein ratio, it can be estimated that the remaining lipids are sufficient to form at least one further lipid shell around the rhodopsin monomers.

Fluid Lipid Component. The spectral properties of the fluid component from the membranes rather closely resemble those of the aqueous dispersions of the extracted membrane lipids. The spectra of the latter are characteristic of a fluid liquid-crystalline environment such as is found for instance with dipalmitoylphosphatidylcholine bilayers in the L_α phase (Pates et al., unpublished results). The apparent order parameter decreases as the label is stepped down the chain, corresponding to an increasing degree of motional freedom toward the terminal methyl groups. This is in qualitative agreement with the results of ^2H NMR studies [see, e.g., Seelig (1977), Davis (1983), and Seelig & Seelig (1980)], although there are very important quantitative differences between the apparent order parameter profiles, almost certainly because of slow-motion effects and local distortion of the chain conformation about the spin-label group (Lange et al., 1985). The difference in apparent order parameter of the fluid components between membranes and lipids may also be due to slow-motional effects, rather than a true increase in order. Both the latter change

and the increase in effective correlation time (Table II) could arise from the effects of exchange between the fluid and motionally restricted lipid, as mentioned earlier. If this is the case, then the mobility of the fluid lipid resembles even more closely that of the extracted lipids.

Since the total lipid content of the ROS membrane is only sufficient for approximately two shells of lipid surrounding each protein, the motionally restricted lipids must be in dynamic equilibrium with the fluid bilayer environment and are only transiently associated with the protein interface. Spectral simulations for rhodopsin–dimyristoylphosphatidylcholine recombinants have indicated that the exchange rate off the protein surface varies from 1.3×10^7 to 1.9×10^7 s^{-1} over the temperature range 25–40 °C (Ryba et al., 1987), in agreement with the results of Davoust et al. (1983) on ^{14}N–^{15}N spin-label collision frequencies. These values are only slightly slower than the exchange rates due to lateral diffusion in dimyristoylphosphatidylcholine bilayers which are found to be $\nu_{ex} = 4D_T/\langle x^2 \rangle \sim (2.5\text{–}5.6) \times 10^7$ s^{-1} over the same temperature range (Vaz et al., 1985). This suggests a close dynamic coupling of all the lipids in the membrane by exchange.

Mobility of the Motionally Restricted Lipid Component. The spectral analysis of the motionally restricted component demonstrates, as has previous work (Favre et al., 1979; Devaux, 1982; Davoust & Devaux, 1982), that the spin-labeled chains at the rhodopsin–lipid interface are by no means rigidly immobilized but their motion is slow on the ESR time scale. The line widths of the motionally restricted spectral components from all the different spin-label positional isomers have an approximately uniform, smooth temperature dependence, although the experimental scatter in the data is quite large (Figure 3B). In contrast, the outer hyperfine splittings (Figure 3A) have separate, approximately parallel, temperature dependences which differ with position in the chain, most probably due to differences in polarity of the spin-label environment. The positional dependence of A_{max} in Figure 3A resembles the polarity profile for the fluid lipid component given in Figure 6B. In particular, the values for the 14- and 13-positions are very similar, corresponding to the hydrophobic interior of the membrane. Using the calibrations established by Griffith et al. (1974), it is found that the overall value of the change in a_0^{app} between the 14- and 9-positions in Figure 6B correlates reasonably well with the corresponding change in A_{max} in Figure 3A. Thus, it seems likely that the systematic shifts in A_{max} must at least in part be due to differences in polarity and that the polarity profile at the lipid–protein interface is rather similar to that in the fluid bilayer.

The conformity of the values for the effective rotational correlation time of the various positional isomers (Figure 4) therefore suggests that there is no steep mobility gradient for the motionally restricted lipid component. However, it should be remembered that the spread in the data is quite large. Therefore, together with the uncertainty in the polarity gradient, a small mobility gradient cannot be excluded. The exchange rates measured for rhodopsin–dimyristoylphosphatidylcholine recombinants correspond to residence times in the range $(5\text{–}8) \times 10^{-8}$ s^{-1} (Ryba et al., 1987), which are longer than the effective rotational correlation times for the motionally restricted lipid component. Thus, it seems likely that there is also some independent mobility of the lipids next to the protein, in addition to exchange. Since somewhat empirical and inequivalent methods were used for analyzing the motional modes, however, care must be exercised in interpreting the absolute values.

Comparison of the effective rotational correlation times for the motionally restricted and fluid lipid components (Figure 4 and Table II) suggests that the motional rates of the lipid chain segments are reduced by a factor of up to approximately 10 on interacting with the surface of the protein. Although some uncertainty exists because of the approximate nature of the motional analyses used, a significant motional restriction of the lipid mobility by the protein is definitely indicated. In this connection, it is interesting to note that a recent detailed analysis of the ^2H NMR parameters for a different lipid–protein system has come to very similar conclusions. For myelin proteolipid apoprotein–dimyristoylphosphatidylcholine recombinants, the correlation times for all chain motions (chain rotation and fluctuation, and trans–gauche isomerization) were increased by a factor of almost 10 at high protein contents (Meier et al., 1987). A rather more restricted analysis of the ^2H NMR spectra of rhodopsin–lipid recombinants has also indicated the existence of slower chain motions in the presence of the protein (Bienvenue et al., 1982; Deese et al., 1981), although quantitative comparisons are not available in this case.

Order of the Motionally Restricted Lipids. Since the spectra of the motionally restricted lipid component lie in the slow-motional regime of ESR spectroscopy, information about chain ordering can only be obtained from oriented specimens. The configurational order of the chains is then described by an orientational distribution function, $\rho(\theta_i)$, where θ_i is the angle between the ith chain segment axis (or nitroxide z axis) and the ordering axis, i.e., the membrane normal. The conventional order parameter obtained by rapid motional averaging of the spectral anisotropies in the fast-motional regime is related to this orientational distribution by

$$S_i = \int_0^{\pi} (1/2)(3 \cos^2 \theta_i - 1)\rho(\theta_i) \sin \theta_i \, d\theta_i / \int_0^{\pi} \rho(\theta_i) \sin \theta_i \, d\theta_i \quad (7)$$

This connection between the order parameter and distribution function gives a useful method for comparison with the results of ^2H NMR, for which the order parameters of the lipids next to and away from the protein are thought to be averaged by exchange which is rapid on the ^2H NMR time scale.

It was not found possible to produce perfectly oriented samples for the ESR experiments, and therefore, the spectrum corresponding to the unoriented part had to be removed by digital subtraction. Two different subtraction strategies were employed, corresponding to Figures 7 and 8 and to Figure 9, respectively. Both gave consistent results, strongly supporting the methods used. Despite the fact that uncertainties involved in this procedure, and the possible distorting effects of slow-motional components, affected the quality of the final difference spectra, for both the 5- and the 14-positions the results indicate a wide distribution of spin-label orientations, i.e., that the effective order parameter (cf. eq 7) is low. The similarity of the motionally restricted component of 14-SASL for both magnetic field orientations (Figure 9d, h) suggests a very high degree of rotational disorder of the chain segments on the surface of the protein at this position. Previous studies on partially oriented cytochrome oxidase membranes (Jost et al., 1973b) have also suggested a wide orientational distribution for the motionally restricted lipid component, although this was not specifically resolved.

These results are in qualitative agreement with the findings of ^2H NMR, which suggest relatively little influence of integral proteins on the segmental chain order parameters (Seelig et al., 1982; Kang et al., 1979; Bloom & Smith, 1985). Indeed,

a detailed spectral analysis for myelin proteolipid apoprotein recombinants has shown that the protein induces relatively little change in either the chain long axis order parameter or the gauche isomer population (Meier et al., 1987). For rhodopsin recombinants with deuteriated lipids, it has also been found that there is no change in the mean chain order parameter, only an increase in the width of the distribution of order parameters (Bienvenue et al., 1982; Deese et al., 1981). Thus, both the ESR results and the NMR results are in agreement that the lipid chains are disordered on the surface of the protein and that certainly there is no high degree of ordering of the chains by the protein.

SUMMARY

The present results show that the mobility of the spin-labeled lipids is restricted along the entire length of the chain, on interaction with the intramembranous surface of rhodopsin. The rate of segmental motion is reduced by a factor of up to 10, but there is no large increase in chain order. These results are in good agreement with those obtained from ^2H NMR, which has a very different characteristic time scale. The absolute values of the estimated rates of chain motion and of the degree of chain order will certainly be affected by the presence of the spin-label group on the chain. However, the consistency of the results between eight different positional isomers suggests that the qualitative changes are insensitive to the exact nature of the probe. In particular, the estimates of the number of lipids directly influenced by the protein are expected to be rather reliable.

ACKNOWLEDGMENTS

We thank Dr. P. J. Brophy of the Department of Biological Sciences, University of Stirling, for performing the fatty acid analyses and Frau B. Angerstein and Dr. A. Watts for the spin-label synthesis.

REFERENCES

Baldwin, P. A., & Hubbell, W. L. (1985) *Biochemistry 24*, 2624–2639.

Baroin, A., Thomas, D. D., Osborne, B., & Devaux, P. F. (1977) *Biochem. Biophys. Res. Commun. 78*, 442–447.

Bienvenue, A., Bloom, M., Davis, J. H., & Devaux, P. F. (1982) *J. Biol. Chem. 257*, 3032–3038.

Bloom, M., & Smith, I. C. P. (1985) in *Progress in Protein–Lipid Interactions* (Watts, A., & De Pont, J. J. H. H. M., Eds.) Vol. 1, pp 61–88, Elsevier, Amsterdam.

Brett, M., & Findlay, J. B. C. (1979) *Biochem. J. 177*, 215–223.

Cone, R. A. (1972) *Nature (London), New Biol. 236*, 39–43.

Daemen, F. J. M. (1973) *Biochim. Biophys. Acta 300*, 255–288.

Davis, J. H. (1983) *Biochim. Biophys. Acta 737*, 117–171.

Davoust, J., & Devaux, P. F. (1982) *J. Magn. Reson. 48*, 475–494.

Davoust, J., Seigneuret, M., Herve, P., & Devaux, P. F. (1983) *Biochemistry 22*, 3146–3151.

Deese, A. J., Dratz, E. A., Dahlquist, F. W., & Paddy, M. R. (1981) *Biochemistry 20*, 6420–6427.

Devaux, P. F. (1982) *Methods Enzymol. 81*, 703–709.

Ebrey, T. G. (1971) *Proc. Natl. Acad. Sci. U.S.A. 68*, 713–716.

Eibl, H., & Lands, W. E. M. (1969) *Anal. Biochem. 30*, 51–57.

Ellena, J. F., Pates, R. D., & Brown, M. F. (1986) *Biochemistry 25*, 3742–3748.

Favre, E., Baroin, A., Bienvenue, A., & Devaux, P. F. (1979) *Biochemistry 18*, 1156–1162.

Folch, J., Lees, M., & Sloane-Stanley, G. H. (1957) *J. Biol. Chem. 226*, 497–509.

Freed, J. H. (1976) in *Spin Labelling. Theory and Applications* (Berliner, L. J., Ed.) Vol. I, pp 53–132, Academic Press, New York.

Griffith, O. H., & Jost, P. C. (1976) in *Spin Labelling. Theory and Applications* (Berliner, L. J., Ed.) Vol. I, pp 453–521, Academic Press, New York.

Griffith, O. H., Dehlinger, P. J., & Van, S. P. (1974) *J. Membr. Biol. 15*, 159–192.

Jost, P. C., Griffith, O. H., Capaldi, R. A., & Vanderkooi, G. A. (1973a) *Proc. Natl. Acad. Sci. U.S.A. 70*, 4756–4763.

Jost, P. C., Griffith, O. H., Capaldi, R. A., & Vanderkooi, G. A. (1973b) *Biochim. Biophys. Acta 311*, 141–152.

Kang, S. Y., Gutowsky, H. S., Hsung, J. C., Jacobs, R., King, T. W., Rice, D., & Oldfield, E. (1979) *Biochemistry 18*, 3257–3267.

Lange, A., Marsh, D., Wassmer, K.-H., Meier, P., & Kothe, G. (1985) *Biochemistry 24*, 4383–4392.

Lowry, O. H., Rosebrough, N. J., Farr, A. L., & Randall, R. J. (1951) *J. Biol. Chem. 193*, 265–275.

Marsh, D. (1985) in *Progress in Protein–Lipid Interactions* (Watts, A., & De Pont, J. J. H. H. M., Eds.) Vol. 1, pp 143–172, Elsevier, Amsterdam.

Marsh, D. (1986) in *Supramolecular Structure and Function* (Pifat-Mrzjlak, G., Ed.) pp 48–62, Springer-Verlag, Heidelberg.

Marsh, D., & Watts, A. (1982a) in *Lipid–Protein Interactions* (Jost, P. C., & Griffith, O. H., Eds.) Vol. 2, pp 53–156, Wiley-Interscience, New York.

Marsh, D., & Watts, A. (1982b) *Methods Enzymol. 88*, 762–772.

Marsh, D., Watts, A., Pates, R. D., Uhl, R., Knowles, P. F., & Esmann, M. (1982) *Biophys. J. 37*, 265–274.

Meier, P., Sachse, J.-H., Brophy, P. J., Marsh, D., & Kothe, G. (1987) *Proc. Natl. Acad. Sci. U.S.A.* (submitted for publication).

Miljanich, G. P., Brown, M. F., Mabrey-Gaud, S., Dratz, E. A., & Sturtevant, J. M. (1985) *J. Membr. Biol. 85*, 79–86.

O'Brien, D. F., Costa, L. F., & Ott, R. A. (1977) *Biochemistry 16*, 1295–1303.

Papermaster, D. S., & Dreyer, W. J. (1974) *Biochemistry 13*, 2438–2444.

Pates, R. D., Watts, A., Uhl, R., & Marsh, D. (1985) *Biochim. Biophys. Acta 814*, 389–397.

Pates, R. D., Ellena, J. F., & Brown, M. F. (1986) *Biochemistry* (in press).

Poo, M.-M., & Cone, R. A. (1973) *Exp. Eye Res. 17*, 503.

Rousselet, A., & Devaux, P. F. (1978) *FEBS Lett. 93*, 161–164.

Ryba, N., Horvath, L. I., Watts, A., & Marsh, D. (1987) *Biochemistry* (submitted for publication).

Sandermann, H. (1978) *Biochim. Biophys. Acta 515*, 209–237.

Sandermann, H. (1986) in *Progress in Protein–Lipid Interactions* (Watts, A., & De Pont, J. J. H. H. M., Eds.) Vol. 2, pp 197–220, Elsevier, Amsterdam.

Schindler, H., & Seelig, J. (1973) *J. Chem. Phys. 59*, 1841–1850.

Seelig, J. (1977) *Q. Rev. Biophys. 10*, 353–418.

Seelig, J., & Seelig, A. (1980) *Q. Rev. Biophys. 13*, 19–61.

Seelig, J., Seelig, A., & Tamm, L. (1982) in *Lipid–Protein Interactions* (Jost, P. C., & Griffith, O. H., Eds.) Vol. 2, pp 127–148, Wiley-Interscience, New York.

Stone, W. L., Farnsworth, C. C., & Dratz, E. A. (1979) *Exp. Eye Res. 28*, 387-397.
Vaz, W. L. C., Clegg, R. M., & Hallmann, D. (1985) *Biochemistry 24*, 781-786.
Watts, A., Volotovski, I. D., & Marsh, D. (1979) *Biochemistry 18*, 5006-5013.
Watts, A., Davoust, J., Marsh, D., & Devaux, P. F. (1981) *Biochim. Biophys. Acta 643*, 673-676.

Parallax Method for Direct Measurement of Membrane Penetration Depth Utilizing Fluorescence Quenching by Spin-Labeled Phospholipids†

Amitabha Chattopadhyay and Erwin London*
Department of Biochemistry, State University of New York at Stony Brook, Stony Brook, New York 11794-5215
Received June 20, 1986; Revised Manuscript Received September 23, 1986

ABSTRACT: This report describes a method suitable for determining the depth of a wide variety of fluorescent molecules embedded in membranes. The method involves determination of the parallax in the apparent location of fluorophores detected when quenching by phospholipids spin-labeled at two different depths is compared. By use of straightforward algebraic expressions, the method allows calculation of depth in angstroms. Furthermore, the analysis can be extended to quenching by energy-transfer acceptors or brominated probes under appropriate conditions. Application of the method to quenching of 7-nitro-2,1,3-benzoxadiazol-4-yl (NBD)-labeled lipids by spin-labeled lipids located at three different depths is demonstrated in model membranes. It is shown that the calculated depths of the NBD groups are self-consistent to the extent that they are the same no matter which two spin-labels have been used in a particular experiment. In addition, the calculated depth is independent of spin-label concentration in the membrane within ±1 Å, ruling out major effects due to spin-label perturbation. The quenching experiments show that the location of the NBD group in head-group-labeled phosphatidylethanolamine is at the polar/hydrocarbon interface and that of an NBD label on the "tail" of cholesterol is deeply buried, as expected. Unexpectedly, NBD labels placed at the end of fatty acyl chains of phosphatidylcholines are also near the polar/hydrocarbon interface. Presumably, the polarity of the NBD group results in "looping" back to the surface of the NBD groups attached to flexible acyl chains.

One of the most important questions in the study of biological membrane structure is the membrane penetration depth, i.e., how far a molecule or a specific site within a molecule is from the membrane surface. Knowledge of the precise depth of a molecule or group should help define the conformation and topology of fluorescent probes and membrane proteins. Fluorescence has been one of the most widely used techniques to determine depth. Most studies have made use of dipole–dipole (Förster) energy transfer [e.g., see Shaklai et al. (1977), Koppel et al. (1979), Fleming et al. (1979), Dewey & Hammes (1980), Sklar et al. (1980), Baird & Holowka (1985), Holowka et al. (1985), Kleinfeld (1985), Kleinfeld & Lukacovic (1985), Davenport et al. (1985), and Hasselbacher et al. (1986)]. However, the analysis of depth in this way has proven to be somewhat complex. Other approaches have involved use of fluorescence quenching by spin-labels [see reviews by London (1982) and Blatt & Sawyer (1985)] or by brominated probes (Kao et al., 1978; Markello et al., 1985; Jain et al., 1985). Spin-labels have the advantage of being quenchers of a wide range of fluorophores, while brominated groups on lipids are relatively small, and probably the least perturbing of the quenchers (East & Lee, 1982). However, attempts to determine precise depth by spin-labels or brominated probes have tended to be more qualitative because, unlike energy transfer, theoretical expressions describing the distance dependence of quenching by these latter probes have been lacking. In this study, we have derived relatively simple mathematical expressions that are applicable to all types of quenching, including that by energy-transfer acceptors. The equations obtained allow straightforward and direct determination of membrane depth in angstroms by comparing the quenching obtained with quenchers at two different depths, i.e., by the apparent degree of parallax in fluorophore position as viewed by quenchers at two different depths.

The method has been tested by examining the location of the fluorescent groups in a series of 7-nitro-2,1,3-benzoxadiazol-4-yl (NBD)[1]-labeled lipids using quenching by spin-labels. Various NBD-labeled lipids have been commonly used as fluorescent lipid analogues [e.g., see Nichols (1985) and Pagano & Sleight (1985)], and closely related probes have

† This work was supported by National Institutes of Health Grant GM 31986. A preliminary version of some of the results in this report was presented at the 30th Annual Meeting of the Biophysical Society, San Francisco, CA, Feb 9-13, 1986.
* Address correspondence to this author.

[1] Abbreviations: NBD, 7-nitro-2,1,3-benzoxadiazol-4-yl; 5 spin-labeled PC, 1-palmitoyl-2-(5-doxyl)stearoyl-*sn*-glycero-3-phosphocholine; 10 spin-labeled PC, 1-palmitoyl-2-(10-doxyl)stearoyl-*sn*-glycero-3-phosphocholine; 12 spin-labeled PC, 1-palmitoyl-2-(12-doxyl)stearoyl-*sn*-glycero-3-phosphocholine; 6-NBD-PC, 1-palmitoyl-2-[6-[(7-nitro-2,1,3-benzoxadiazol-4-yl)amino]caproyl]-*sn*-glycero-3-phosphocholine; 12-NBD-PC, 1-palmitoyl-2-[12-[(7-nitro-2,1,3-benzoxadiazol-4-yl)-amino]dodecanoyl]-*sn*-glycero-3-phosphocholine; NBD-PE, *N*-(7-nitro-2,1,3-benzoxadiazol-4-yl)dipalmitoyl-*sn*-glycero-3-phosphoethanolamine; NBD-cholesterol, 25-(NBD-methylamino)-27-norcholesterol; DOPC, dioleoyl-*sn*-glycero-3-phosphocholine; Tempol, 4-hydroxy-2,2,6,6-tetramethylpiperidinyl-1-oxy; TPC, 2,2,5,5-tetramethyl-3-pyrroline-1-oxyl-3-carboxy acid; TLC, thin-layer chromatography; ESR, electron spin resonance.

0006-2960/87/0426-0039$01.50/0